PERGAMON

International Journal of Heat and Mass Transfer 42 (1999) 1479–1489

International Journal of HEAT and MASS TRANSFER

Interfacial breakdown of double-diffusive convective layers by a horizontal temperature gradient

Tatsuo Nishimura[a,*], Yasuyuki Ogata[a], Soshun Sakura[a], Alexandru M. Morega[b]

[a] *Department of Mechanical Engineering, Yamaguchi University Ube, 755-8611 Japan*
[b] *Department of Electrical Engineering, Politechnica University of Bucharest, Bucharest, 77206 Romania*

Received 17 February 1998; in final form 5 June 1998

Abstract

A two-layer, salt-stratified system destabilized and mixed by lateral heating and cooling is studied experimentally using three different enclosures. The following conditions are considered: thermal Rayleigh number $Ra_T = 2\times10^7$–7×10^8 and initial buoyancy ratio $N_i = 0.441$–0.882. Kelvin–Helmholtz vortices occur, in the initial stages before mixing, within the interface that separates the top and bottom convective layers due to shear instabilities. After that, the interface is significantly tilted and is rolled up near the hot and cold walls, while following the downward migration of the interface at the cold wall, the fluid in the bottom layer penetrates into the top layer along the hot wall, indicating the onset of mixing. These mixing processes depend on the thermal Rayleigh number and initial buoyancy ratio. Finally we propose a correlation for the dimensionless mixing time, valid for initial buoyancy ratios less than unity.

Nomenclature

A geometric aspect ratio of enclosure ($= H/L$)
C concentration
C_1 initial lower concentration fluid in the top layer
C_2 initial higher concentration fluid in the bottom layer
C_m mixed concentration ($=(C_1+C_2)/2$)
c dimensionless concentration ($=(C-C_m)/\Delta C$)
D species diffusivity
d diffusion thickness
Fo_m dimensionless mixing time defined by eqn (3)
g gravitational acceleration
H height of enclosure
L length of enclosure
Le Lewis number ($=\alpha/D$)
N initial buoyancy ratio defined by eqn (2)
Pr Prandtl number ($=\nu/\alpha$)
Ra_T thermal Rayleigh number defined by eqn (1)
Sc Schmidt number ($=\nu/D$)
T temperature
T_c cold wall temperature
T_h hot wall temperature
T_i initial temperature ($=(T_h+T_c)/2$)
t time
t_d diffusion time
t_m mixing time
x horizontal coordinate
w width of enclosure
z vertical coordinate.

Greek symbols
α thermal diffusivity
β_c compositional expansion coefficient
β_t thermal expansion coefficient
ΔT temperature difference ($=T_h-T_c$)
ΔC concentration difference ($=C_2-C_1$)
ν kinematic viscosity.

1. Introduction

Natural convection due to spatial variations of fluid density is of fundamental importance in many natural

* Corresponding author. Tel.: +81 846 35 9909; Fax: +81 836 35 9926; E-mail: tnishimu@mechgw.mech.yamaguchi-u.ac.jp

0017–9310/98/$ - see front matter
PII: S0017–9310(98)00205–1

and industrial problems. Recently, it was noticed an increased interest in the role that double-diffusive natural convection plays in crystal growth techniques specific to semiconductors and solidification processes of metallic alloys [1–6]. A number of the experimental and numerical studies on solidification of binary systems revealed the formation, interaction and merging of vertically-stacked, horizontal convective layers due to lateral heating or cooling in a stably stratified solution [7–9]. The occurrence and development of the layers in a supereutectic NH_4Cl–H_2O system was studied experimentally by Nishimura et al. [10]. They found that criteria for layer formation depend on the buoyancy ratio and the thermal Rayleigh number in the diffusive interface between two layers, and that the stability conditions are analogous to those for double-diffusion without phase change, determined by Chen et al. [11].

On the other hand, the mechanism of layer merging has not been well known even at the present time. Nishimura et al. [12] examined the solidification process of a NH_4Cl–H_2O system and found that the diffusive interface between two layers is kinematically unstable when the buoyancy ratio at the onset of layer merging is less than unity and the corresponding thermal Rayleigh number is of the order of 10^6.

A few studies regarded the layer merging without phase change. Bergman and Ungan [13] performed an experimental investigation of double-diffusive convection in a two-layer, salt-stratified NaCl–H_2O system destabilized by lateral heating and cooling, for initial buoyancy ratios near unity. Flow visualization revealed that the convective structure of the system is very complex, and that the dimensionless mixing time depends on the thermal Rayleigh number and the initial buoyancy ratio. Yamane et al. [14] carried out similar experiments for a Na_2CO_4–H_2O system. The dimensionless mixing time was found to be inversely proportional to the temperature difference under a fixed value of the vertical concentration difference. This result is different from the one reported by Bergman et al. [13]. The main reasons for this discrepancy are probably due to the definition of the mixing time as well as the specific initial state of the diffusive interface between convective layers. They defined the mixing time using flow visualization by particle tracers, a technique that berries uncertainties and, therefore quantitative estimations such as temperature and concentration measurements are needed. Furthermore, numerical simulations have been performed in this system. Hyun and Bergman [15] studied numerically, using a Chebyshev collocation method, the physical process leading to the layer merging in a square cavity. The agreement between their predicted and measured mixing times was not satisfactory: the measured value is two times the predicted one. Kamakura and Ozoe [16] studied the layer merging in a tall enclosure using the finite element method, but they did not perform a direct comparison with the experiments. Although not directly related to the present work, Beckermann [17, 18] performed both experimentally and numerically a two-layer stratified system in a Hele–Shaw cell (two-dimensional cell), and the agreement in the concentration field was satisfactory. However, the detailed flow structure would be quite different between two and three-dimensional cells. Accordingly, there is a great lack of information on the mixing time representing the overall behavior in a two-layer, salt-stratified system. The present experimental study focuses on the mixing process in a two-layer, salt-stratified NaCl–H_2O system destabilized by lateral heating and cooling, with varying several parameters.

2. Experimental apparatus and procedure

Experiments were performed using rectangular enclosures of three different sizes. The geometric aspect ratio and the depth of the enclosures were fixed ($A = 1.25$ and $W = 170$ mm) and the height, H and horizontal length of the enclosure, L were 78×62.4 mm, 114×91.2 mm and 150×120 mm. Respective enclosures are called small, medium and large ones. Figure 1 illustrates a schematic of the experimental apparatus. Its main parts are the cooling, the testing and the heating sections. The test section was a rectangular enclosure made of an acrylic resin (15 mm thick), placed between two copper plates (5 mm thick) that correspond to the hot and cold walls. Several thermocouples for continuous temperature monitoring, were imbedded in the hot and cold walls. Each wall was attached to a heat exchanger that was connected to four loops through which the flow rate of coolant could be controlled independently. The heat exchangers were connected to constant-temperature baths through a valve system. Water was used as the coolant in these baths. The experimental apparatus was covered with styroform insulating material 60 mm thick in order to minimize heat loss. Two removable windows in the insulation allowed for illumination and visual observations.

The rectangular enclosure was step-wisely filled with two layers of water with uniform salinity by carefully introducing a higher concentration layer below a lower concentration layer. The volumes of the two layers were identical, and in order to perform the experiments for small buoyancy ratios, the initial concentration difference was varied from 0.2–0.8 wt% under a fixed value of the mixed concentration after layer merging, i.e., $C_m = 1.0$ wt%. At the beginning of each experiment, the interface at mid-height was observed to be very sharp (thickness of order 1 mm).

The experiments were performed in a temperature-controlled environmental chamber, set at 20°C. The initial temperature of two-layer, salt-stratified fluid T_i was established midway between the hot and cold wall temperatures and it was always 20°C. A test run was

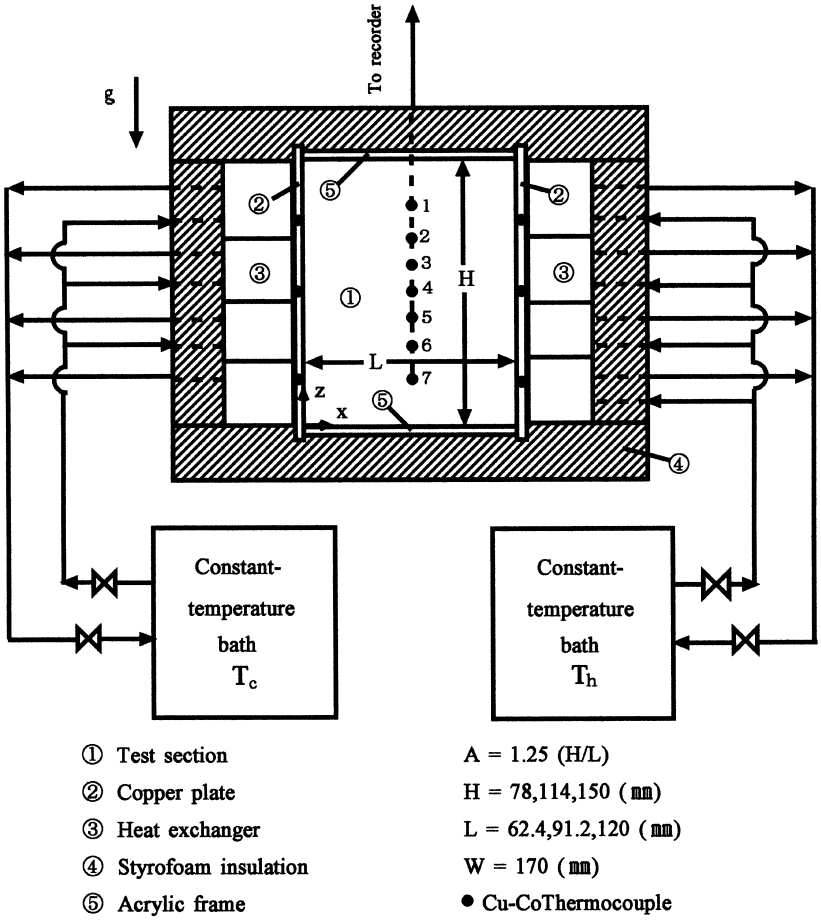

Fig. 1. Experimental apparatus.

initiated by simultaneously changing the temperatures of coolants in the two heat exchangers. The temperature difference between the hot and cold walls was varied from 8 to 35°C. The thermal Rayleigh number and the initial buoyancy ratio governing the system behavior are defined through

$$Ra_T = \frac{g\beta_T \Delta T L^3}{\nu\alpha} \tag{1}$$

$$N_i = \frac{\beta_c \Delta C}{\beta_T \Delta T} \tag{2}$$

The fluid properties in these parameters are estimated with the average temperature and concentration of the fluid. In this experiment, these parameters are in the ranges, $2\times10^7 < Ra_T < 7\times10^8$ and $0.441 < N_i < 0.882$, respectively.

Flow visualizations using tracers such as liquid crystal particles with an average diameter of 25 μm and Rhodamine B dye were performed to examine the layer merging during the experiment. Since the molecular diffusivities of salt and Rhodamine B are approximately the same, the changes in the salt concentration could be monitored by tracking the concentration of Rhodamine B. Qualitative flow visualization was performed using the laser-induced fluorescence technique as an initial step of the experiments for the layer merging. The Rhodamine dye fluoresces at 570 nm when exposed to 514 nm emission of the argon-ion laser. The measurements of the bulk temperature in the enclosure were made with copper–constantan thermocouples of 100 μm in diameter, placed in a plastic tube with an o.d. of 2 mm. These probes were inserted through 7 holes located in the back wall of the enclosure. The concentration in the fluid was also measured by a conductivity probe.

3. Results and discussion

3.1. *Diffusion time*

Because a steplike concentration profile is difficult for experiments, we first examine the initial state of the

diffusive interface between convective layers. Figure 2 shows vertical concentration profiles at $x/L = 0.5$ for two different moments. Here the time is measured from the moment when a higher concentration layer is introduced below a lower concentration layer. The experimental data are measured by a single-electrode conductivity probe, while the theoretical curves are obtained analytically [19]. The agreement between the theoretical and experimental concentrations is very satisfactory. As time proceeds, the concentration profile exhibits a smooth variation and the diffusive thickness becomes large near the interface, i.e., $d = (8Dt_d)^{1/2}$. Thus, it seems that the diffusion time prior to the application of the thermal boundary conditions of heating and cooling influences the mixing time for the layer merging.

Figure 3 shows flow visualization photographs by the laser-induced fluorescence technique for two diffusion times, i.e., $t_d = 40$ and 400 min. In this figure, the time is measured from the beginning of heating and cooling. Although the mixing processes are qualitatively similar except in the early stages of the experiment, the onset of mixing occurs faster for larger diffusion time, as shown in Fig. 4. Here t_m denotes the mixing time, defined later. In the present study, considering the time required for the formation of a two-layer, salt-stratified system, diffusion time is fixed at $t_d = 60$ min. Thus, the mixing time appears to be a few percents lower than that of a step-like concentration profile.

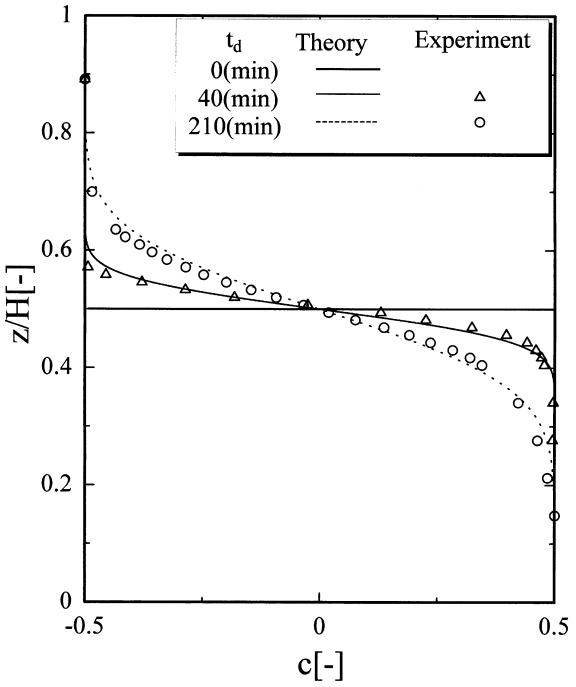

Fig. 2. Theoretical and experimental concentration profiles at two diffusion times.

3.2. Flow patterns and mixing processes

Thirty seven experiments with various thermal Rayleigh numbers and initial buoyancy ratios were performed, for Prandtl and Lewis number 7.15 and 95.9, respectively, and for the conditions $T_i = 20°C$ and $C_m = 1.0$ wt%.

Since, as reported by Bergman et al. [13], the general flow patterns prior to mixing are classified into quasi-steady and unsteady regimes, we pay attention to the flow near the diffusive interface between the convective layers. Here, the circulation in each layer experiences counterclockwise rotation. Figure 5 (a) shows sample photographs about $t = 85$ min in the quasi-steady regime for a small enclosure. The exposure time is 4 s. From particle paths, we observe boundary layer flows along the hot and cold walls and counter shear flows separated by the interface. The interface is slightly tilted due to the horizontal temperature gradient and its thickness is about 1 mm. No fluid appears directly to penetrate the interface between the top and bottom layers. Each shear flow is developed along the interface. That is, above the interface, the velocity along the interface is accelerated towards the hot wall, while below the interface the acceleration reverses. Secondary circulation is evident on the upper-right and lower-left of the interface. Thus, the flow keeps symmetric behavior about the diagonal of the enclosure.

Figure 5 (b) shows photographs about $t = 123$ min in the early stages of the unsteady regime. These photographs are not taken simultaneously. The interface is more tilted, and four small Kelvin–Helmholtz vortices with clockwise rotation marked by *a*, *b*, *c*, and *d* are generated due to shear instabilities, within the interface. The vortices *a* and *b* move towards the cold wall, while the vortices *c* and *d* move towards the hot wall. Vortex motion depends on the velocity difference between the top and bottom layers near the interface. That is, the vortices are pulled in the direction of shear flow with a larger velocity.

Figure 5(c) shows photographs about $t = 163$ min, just before the layer merging. Because of the interface tilting, a lower concentration fluid of the top layer and a higher concentration fluid of the bottom layer cover over the cold and hot walls, respectively, while asymmetric behavior is observed. After that, the higher concentration fluid overlies the lower concentration fluid, leading to an unstable state.

Next we describe the mixing processes. Figure 6 shows the time history of concentration at the center of the top layer corresponding to the flow visualizations of Fig. 5. The concentration gradually increases during the quasi-steady and unsteady regimes, indicating mass transfer across the interface. However, at the end of the unsteady regime, a sudden increase in the concentration is observed. Figure 7 shows flow visualizations using the

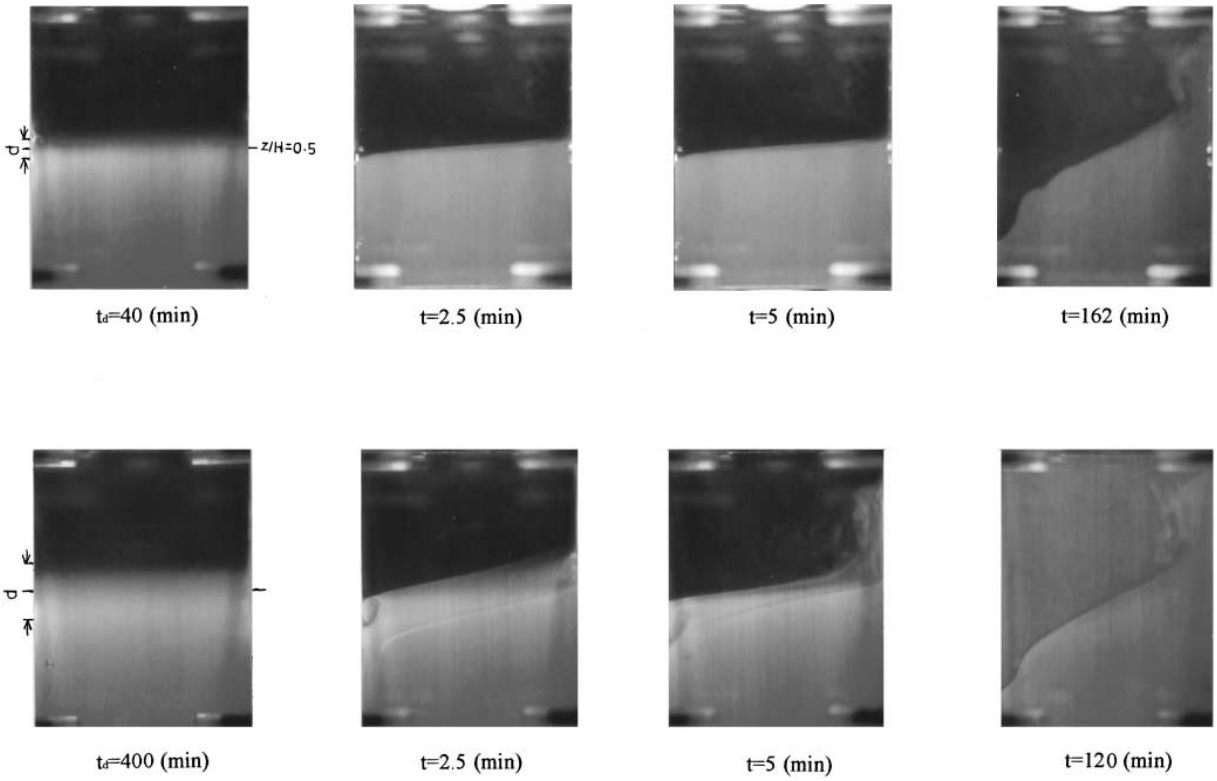

Fig. 3. Visualizations of mixing process for two diffusion times for $Ra_T = 2.7 \times 10^7$ and $N_i = 0.882$.

laser-induced fluorescence technique for three cases. Since the mixing behavior during the quasi-steady and unsteady regimes is similar for all cases, only one photograph is shown as an example, i.e., namely when Kelvin–Helmholtz vortices exist within the interface. The interface is undulated and it varies with time. Past the end of the unsteady regime, the mixing process depends on the thermal Rayleigh number and initial buoyancy ratio. We notice that the interface near the central part is smooth again, indicating the disappearance of Kelvin–Helmholtz vortices. Furthermore, we observe that the interfacial breakdown is induced by the interface roll-up, or local fluid penetration. For case (a), the roll-up of the interface is observed at the hot and cold walls indicating a weak asymmetry; furthermore, when a higher concentration fluid overlies a lower concentration fluid salt fingers are observed. For case (b), asymmetric behavior due to a higher temperature difference becomes even more remarkable. On the other hand, the breakdown of the interface is observed at the hot wall for case (c), indicating that a higher concentration fluid along the hot wall in the bottom layer penetrates into the top layer. Consequently, the interface near the cold wall migrates downward due to continuity of fluid. Thus, asymmetric behavior is found to be observed near the interfacial breakdown and it is attributed to the variation in the thermal properties with temperature.

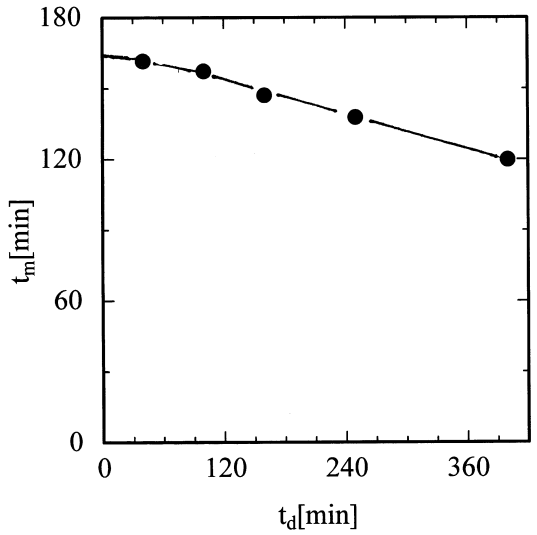

Fig. 4. Mixing time vs diffusion time for $Ra_T = 2.7 \times 10^7$ and $N_i = 0.882$.

Figure 8 shows the temperature histories for three different heights corresponding to the mixing processes

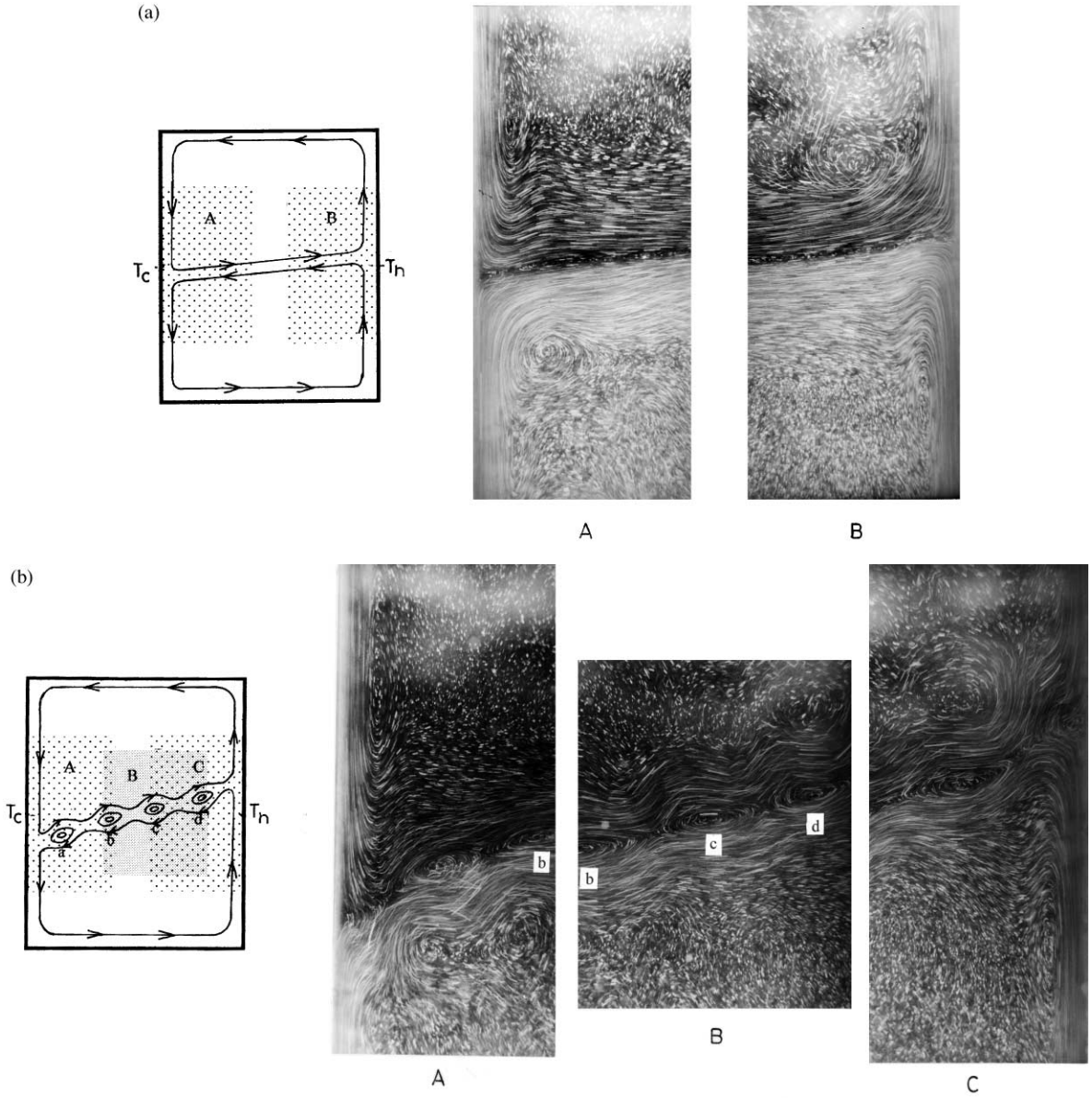

Fig. 5. *Caption opposite*.

of Fig. 7. In each case, at the onset of the roll-up of the tilting interface and fluid penetration, the temperatures change suddenly, to eventually reach the steady state specific to purely thermal convection. Therefore, in the present study, the mixing time for layer merging is defined as the moment when the temperature at the position 1 in the top layer suddenly changes, in contrast to the definition given by Bergman et al. [13] who stated it as the time when relative motion of the tracer particles could no longer be distinguished. Figure 9 shows the diagram representing three mixing processes (see Fig. 7) for three different enclosures. The dotted line denotes the boundary between symmetric and asymmetric behaviors of the interface roll-up, while the solid line is the boundary between the interface roll-up and the fluid penetration for the interfacial breakdown. We find that the roll-up of the interface takes place at lower thermal Rayleigh numbers, while the fluid penetration occurs at high thermal Rayleigh numbers, depending on the initial buoyancy ratio.

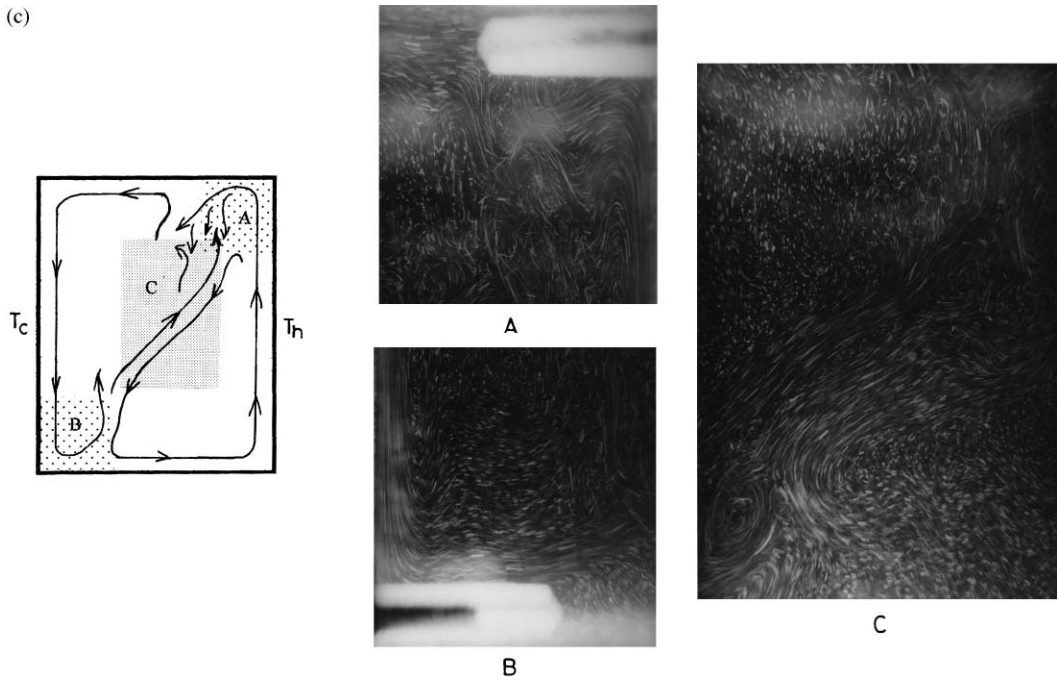

Fig. 5. Flow visualizations by particle path about (a) $t = 85$ min, (b) $t = 123$ min and (c) $t = 163$ min for $Ra_T = 2.7 \times 10^7$ and $N_i = 0.882$.

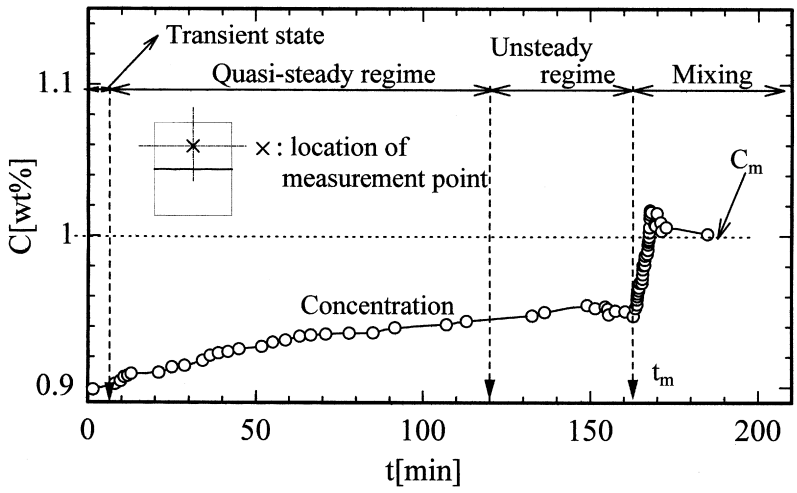

Fig. 6. Time history of concentration at the center of the top layer for $Ra_T = 2.7 \times 10^7$ and $N_i = 0.882$.

3.3. Mixing time

Figure 10 shows the variation of the mixing time defined above with the initial concentration difference between the top and bottom layers, under a fixed temperature difference. The mixing time increases linearly with the concentration difference and its gradient increases as the enclosure size is larger. Figure 11 shows also the temperature difference effect. The mixing time decreases when increasing the temperature difference, and a linear relationship is shown by a semi-logarithmic plot. This result is different from the one reported by Yamane et al. [14]. The dimensionless mixing time is defined as

$$Fo_m = \frac{Dt_m}{L^2} \tag{3}$$

In Fig. 12, we plot the dimensionless mixing time as a

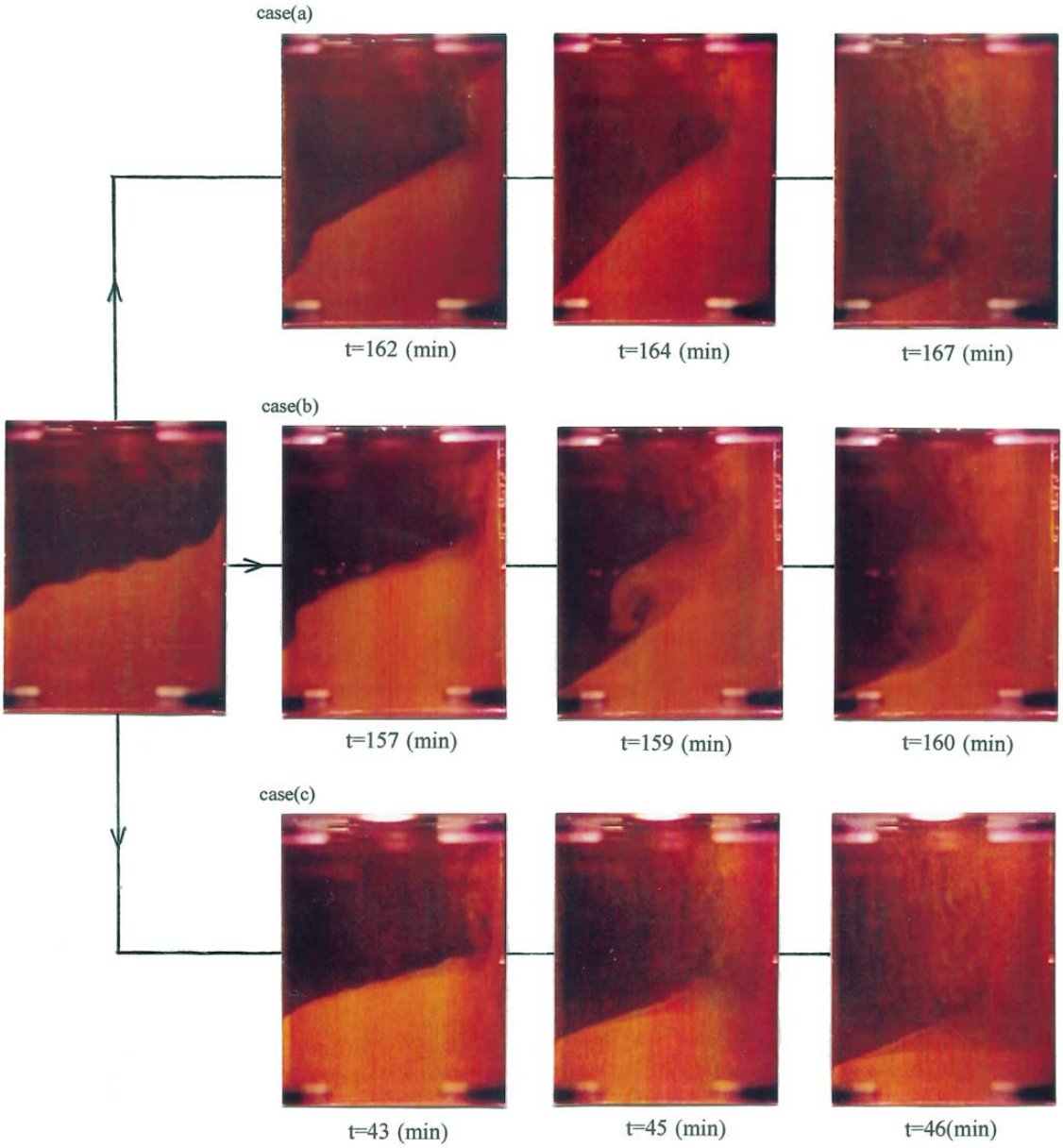

Fig. 7. Mixing processes after the unsteady regime for three cases (a) $Ra_T = 2.7 \times 10^7$ and $N_i = 0.882$, (b) $Ra_T = 5.4 \times 10^7$ and $N_i = 0.882$, (c) $Ra_T = 7.1 \times 10^7$ and $N_i = 0.504$.

function of the initial buoyancy ratio. Although a linear relationship is noticed for all cases, its gradient depends on the enclosure size and the concentration difference, in other words the temperature difference. Considering the result of Fig. 11, we replot in Fig. 13 the mixing time vs logarithms of the thermal Rayleigh number. Despite the scatter in the experimental data, a linear relationship is obtained for a fixed initial buoyancy ratio. Therefore, the dimensionless mixing time is correlated with the initial buoyancy ratio and the thermal Rayleigh number and the correlation is given by,

$$Fo_m = (-0.172 \ln Ra_T + 5.9 N_i + 1.156) \times 10^{-3} \quad (4)$$

The uncertainty in this correlation includes an error of

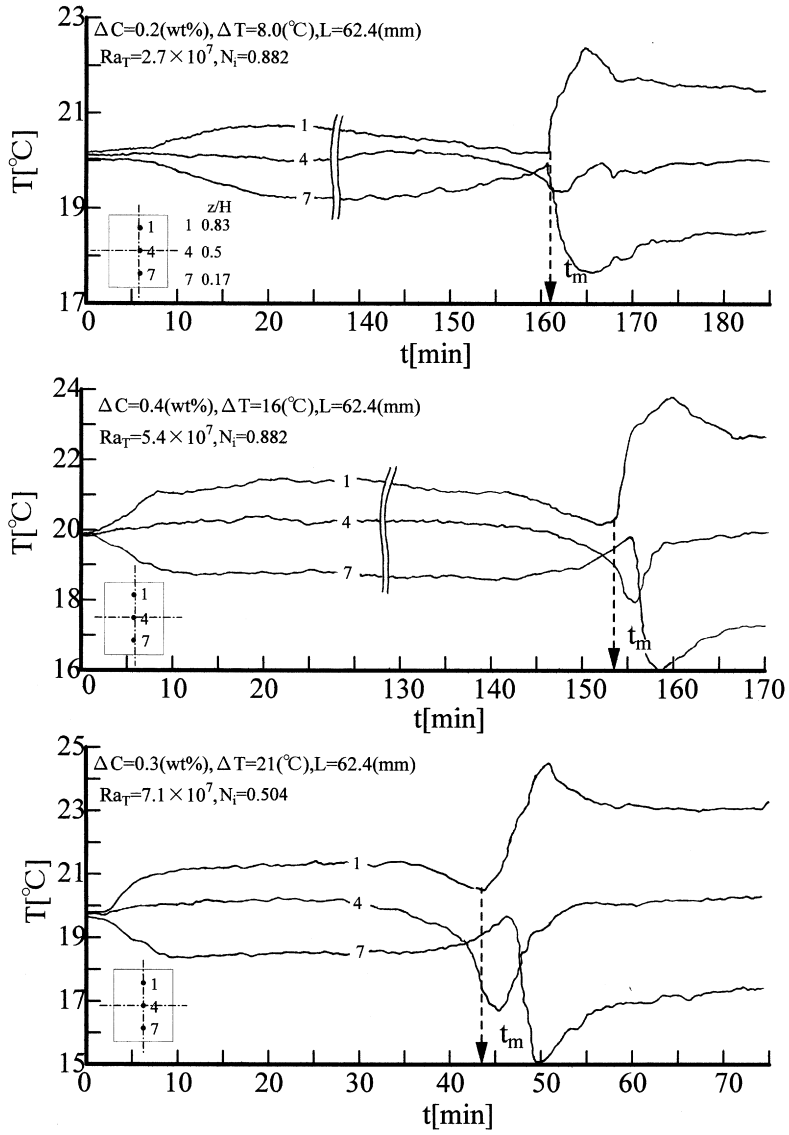

Fig. 8. Time histories of temperatures for three cases.

6%, which is attributed to the different mixing processes as shown in Fig. 9.

4. Conclusions

We studied a two-layer, salt-stratified system destabilized and mixed by lateral heating and cooling. The experiments were performed in the ranges, $2\times10^7 < Ra_T < 7\times10^8$ and $0.441 < N_i < 0.882$. The following conclusions have been drawn:

(1) Kelvin–Helmholtz vortices are generated within the interface due to shear instabilities in this experimental range and they move towards the hot and cold walls, respectively. However, as the interface is furthermore tilted, they eventually vanish.

(2) The interfacial breakdown is induced by the roll-up of the interface, or the fluid penetration along the hot wall which depends on the thermal Rayleigh number and the initial buoyancy ratio.

(3) The correlation for the mixing time as a function of the thermal Rayleigh number and the initial buoyancy ratio is proposed as follows

$$Fo_m = (-0.172\ln Ra_T + 5.9N_i + 1.156)\times10^{-3}$$

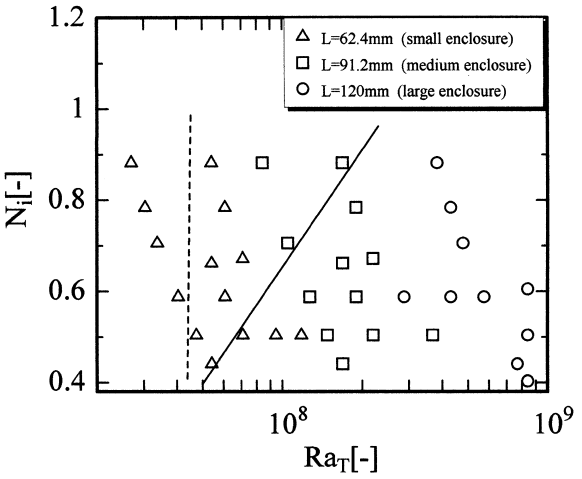

Fig. 9. Diagram of mixing processes in terms of thermal Rayleigh number and initial buoyancy ratio.

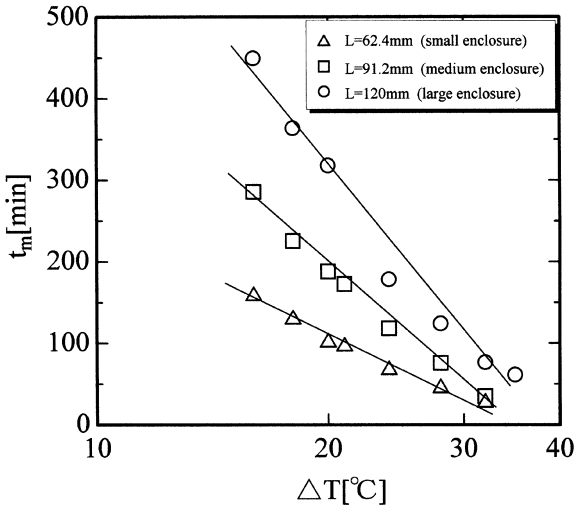

Fig. 11. Mixing time vs temperature difference between hot and cold walls.

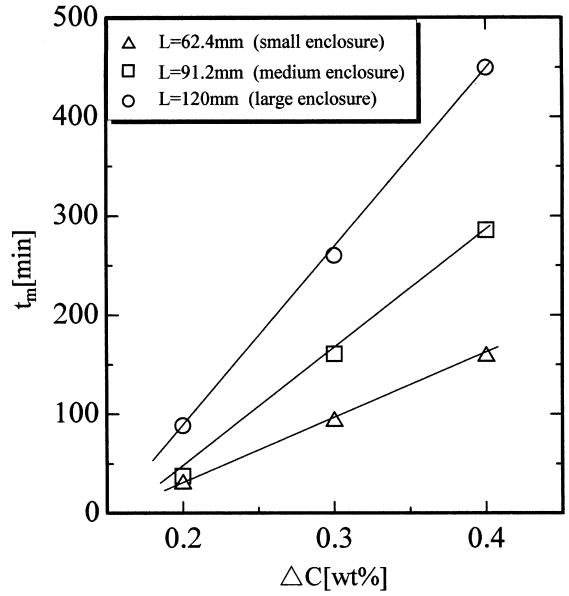

Fig. 10. Mixing time vs concentration difference between top and bottom layers.

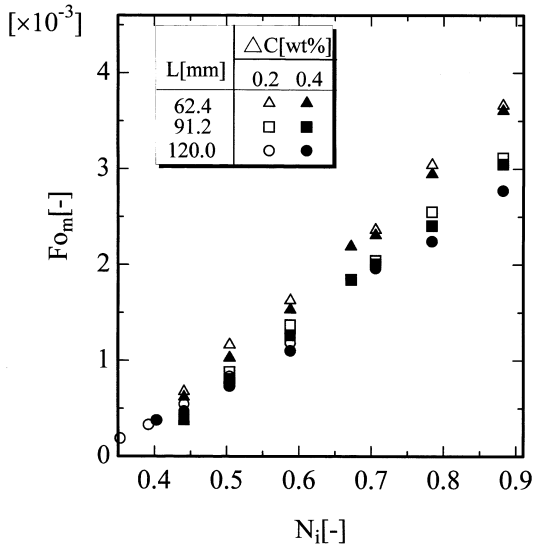

Fig. 12. Dimensionless mixing time vs initial buoyancy ratio.

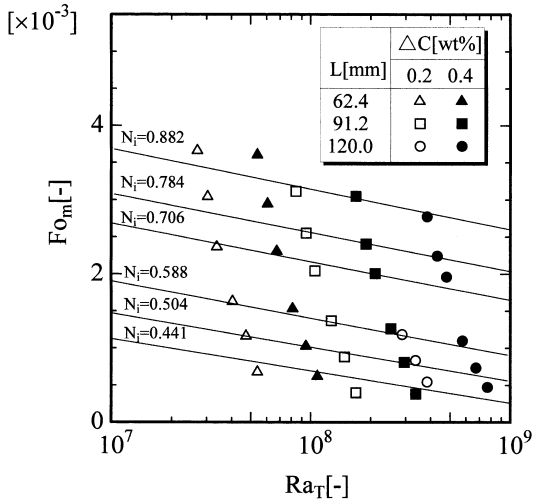

Fig. 13. Dimensionless mixing time vs thermal Rayleigh number for different initial buoyancy ratios.

References

[1] S. Ostrach, Fluid mechanics in crystal growth, J. Fluid Eng. 105 (1983) 5–20.

[2] M.E. Glicksman, S.R. Coriell, G.B. McFadden, Interaction of flows with the crystal-melt surface, Ann. Rev. Fluid Mech. 18 (1986) 307–335.

[3] H.E. Huppert, The fluid mechanics of solidification, J. Fluid Mech. 212 (1990) 209–240.

[4] C. Beckermann, R. Viskanta, Mathematical modeling of transport phenomena during alloy solidification, Appl. Mech. Rev. 46 (1993) 1–27.

[5] A.A. Wheeler, Description of transport processes, in: D.T.J. Hurle (Ed.), Handbook of Crystal Growth, Elsevier Science, Amsterdam, 1993, pp. 683–740.

[6] T. Nishimura, Double-diffusive convection in solidification processes, Kagaku Kogaku 61 (1997) 924–927.

[7] C. Beckermann, R. Viskanta, An experimental study of solidification of binary mixtures with double-diffusive convection in the liquid, Chem. Eng. Comm. 85 (1989) 135–156.

[8] M.E. Thompson, J. Szekely, Mathematical and physical modeling of double-diffusive convection of aqueous solutions crystallizing at a vertical wall, J. Fluid Mech. 186 (1989) 409–433.

[9] T. Nishimura, M. Fujiwara, H. Miyashita, Visualization of temperature fields and double-diffusive convection using liquid crystals in an aqueous solution crystallizing along a vertical wall, Exp. Fluids 12 (1992) 245–250.

[10] T. Nishimura, T. Imoto, H. Miyashita, Occurrence and development of double-diffusive convection during solidification of a binary system, International Journal of Heat and Mass Transfer 37 (1994) 1455–1464.

[11] C.F. Chen, D.G. Briggs, R.A. Wirtz, Stability of thermal convection in a salinity gradient due to lateral heating, International Journal of Heat and Mass Transfer 14 (1971) 57–65.

[12] T. Nishimura, T. Imoto, M. Wakamatsu, Layer merging during solidification of supereutectic NH_4Cl–H_2O system, International Journal of Heat and Mass Transfer 41 (1998) 3669–3674.

[13] T.L. Bergman, A. Ungan, A note on lateral heating in a double-diffusive system, Journal of Fluid Mechanics 194 (1988) 175–186.

[14] T. Yamane, K. Toyama, A. Shiroishi, M. Yoshida, H. Miyashita, Double-diffusive convection of an aqueous solution by lateral heating and cooling, Technical Reports of Toyama University 46 (1995) 99–108.

[15] H.T. Hyun, T.L. Bergman, Direct simulation of double-diffusive layered convection, Journal of Heat Transfer 117 (1995) 334–339.

[16] K. Kamakura, H. Ozoe, Oscillatory double-diffusive natural convection in a two-layer system, Proceedings of the Tenth International Heat Transfer Conference, Brighton, vol. 7, 1994, pp. 67–72.

[17] C. Beckermann, C. Fan, J. Mihailovic, Numerical simulations of double-diffusive convection in a Hele–Shaw cell, International Video Journal of Engineering Research 1 (1991) 71–82.

[18] J. Mihailovic, C. Beckermann, Development of a two-dimensional liquid species concentration measurement technique based on absorptiometry, Exp. Thermal and Fluid Science 10 (1995) 113–123.

[19] E.L. Cussler, Diffusion Mass Transfer in Fluid Systems. Cambridge University Press, Cambridge, 1984.